

## X-RAY ABSORPTION IN POLYMERS\*

H. MORAWITZ, P. BAGUS, T. CLARKE, W. GILL, P. GRANT and G. B. STREET

*IBM Research Laboratory, San Jose, CA 95193 (U.S.A.)*

D. SAYERS

*North Carolina State University, Raleigh, NC 27650 (U.S.A.)*

### Summary

We report on the results of a series of X-ray absorption experiments utilizing synchrotron radiation on the polymeric conductors, brominated  $(\text{SN})_x$ , and  $(\text{CH})_x$  doped with  $\text{AsF}_5$ . These experiments employ the K-edges of bromine and arsenic at 13.47 keV and 11.89 keV, respectively, for the study of the short range order in the vicinity of the source atom. This information is supplied by the backscattering effect of the surrounding coordination shells on the ejected K-shell electron (EXAFS). In addition, the edge region fine structure is studied to deduce information on the molecular species present ( $\text{Br}_2$  or  $\text{Br}_3^-$  in  $(\text{SN})_x$ ,  $\text{AsF}_5$  or  $\text{AsF}_6^-$  in  $(\text{CH})_x$ ).

Experiments were performed over a range of temperatures between 5 K and room temperature to check the relevant distance parameters and charge transfer for their temperature dependence. Nearest and second nearest neighbor distances are given for the bromine species in  $(\text{SN})_x$ , while an average As-F distance for the arsenic species in  $(\text{CH})_x$  is found to be somewhat larger than for  $\text{AsF}_5$  gas molecules.

The advantages of X-ray absorption spectroscopy over other methods such as XPS and UPS for the resolution of chemical questions in partially disordered systems are stressed, particularly, the bulk sensitivity of X-ray absorption *vis-à-vis* the surface escape depth problems of the other techniques.

---

### 1. Introduction

We have recently begun X-ray absorption studies of the molecular species, internal structure, charge transfer, relative position and orientation with respect to the host crystal for a series of molecular dopants such as  $\text{Br}_2$ ,  $\text{I}_2$ ,  $\text{ICl}$  and  $\text{AsF}_5$  in the polymeric conductors  $(\text{SN})_x$  and  $(\text{CH})_x$  [1, 2]. While the former material is conducting in its pristine state [3],  $(\text{CH})_x$  undergoes an insulator-metal transition as a function of dopant concentration for a

---

\*Paper presented at the Symposium on the Structure and Properties of Highly Conducting Polymers and Graphite, San Jose, California, March 29 - 30, 1979.

variety of dopants [4, 5], inducing either electron or hole conduction in the delocalized  $\pi$ -electron framework of the  $(\text{CH})_x$  chains. X-ray absorption spectroscopy has seen rapid expansion in the past five years with the application of intense and continuous synchrotron radiation from storage rings and the rapid development of quantitative theories of extended X-ray absorption fine structure (EXAFS) [6, 7]. The origin of this structural interference effect is the modification of the final electronic state by backscattering from the nearest atomic shells surrounding the source atom. Because of the relatively short mean-free path of electrons with kinetic energies between 50 and 1 500 eV in solids, the backscattering probes distances no further than the fourth or fifth coordination shell ( $\sim 5 \text{ \AA}$ ). On the other hand, as has been stressed in the many applications of EXAFS to ordered and disordered solids and liquids [8 - 10], no requirement for translational invariance has to be met, making the technique a very powerful tool for the study of amorphous and disordered materials.

The possibility of enhancing the conductivity of organic materials has been intensively pursued in graphite with its filled  $\pi$ -valence band and empty  $\pi^*$ -conduction band, which may be partially filled or emptied by the introduction of electron donors or acceptors between the graphite planes. Considerable parallels exist between intercalated graphite on the one hand and  $(\text{SN})_x$  and  $(\text{CH})_x$  exposed to various dopants on the other. Halogens such as  $\text{Br}_2$  and  $\text{I}_2$ , as well as  $\text{ICl}$ , can be introduced into  $(\text{SN})_x$ , and the very reactive  $\text{AsF}_5$  species has been used in both graphite and  $(\text{CH})_x$  [11 - 13].

Some controversy has arisen in the interpretation of a variety of experimental approaches to resolve the question of the molecular species present in graphite and  $(\text{CH})_x$  [14, 15]. The chemically appealing solid state reaction  $3\text{AsF}_5 \rightarrow 2\text{AsF}_6^- + \text{AsF}_3$  has been proposed to occur both in graphite [16] and  $(\text{CH})_x$  [14]. The experiments described in this paper were aimed at resolving these questions by obtaining nearest and second nearest neighbor distances as well as edge structure information from the X-ray absorption spectrum. The obvious advantage of X-ray absorption techniques for the determination of the molecular nature of the dopant species is its bulk nature. This is in marked contrast to other core-level spectroscopies, which detect final state electrons such as UPS or XPS [15]. Due to the short escape depth of the final state electrons, these other experimental approaches are only sensitive to molecular species located in the top 10 - 50  $\text{\AA}$  layer of the material studied and leave the question of the bulk species unanswered. Admittedly, some problems may arise in X-ray absorption experiments on polycrystalline samples due to non-uniform sample thickness or pinhole effects [17]. These effects can, however, in principle be corrected for by using samples of different thickness and studying the orientational dependence of the X-ray absorption for aligned absorbers [18].

The experiments on brominated  $(\text{SN})_x$  will be described in Section 2. Molecular bromine gas and the compound  $\text{S}_4\text{N}_3\text{Br}_3$  [19] were used as standards to determine the phase-shift correction and provide information on the edge structure of  $\text{Br}_2$  and  $\text{Br}_3^-$ . Section 3 presents preliminary results

on  $\text{AsF}_5$  gas phase samples and  $(\text{CH})_x$  exposed to  $\text{AsF}_5$ . Section 4 presents a brief summary on the excitonic structure of cage molecules such as  $\text{AsF}_3$ ,  $\text{AsF}_5$  and  $\text{AsF}_6^-$  on the basis of SCF Hartree-Fock calculations. Section 5 summarizes our results to date and discusses future directions for experiments and theory in this field.

## 2. Bromine in $(\text{SN})_x$

Extensive physical measurements have been performed on the anisotropic conductor  $(\text{SN})_x$  since the discovery of its superconducting transition, aimed at a better understanding of its anisotropic transport properties [3]. Bromination enhances the room temperature conductivity by a factor of 10 and raises the superconducting transition temperature by 10% [20]. The X-ray absorption experiments reported here were undertaken to resolve questions raised by electron diffraction [21], Raman scattering [22], and ir absorption experiments [23] on the molecular nature of the incorporated bromine ( $\text{Br}_2$ ,  $\text{Br}_3^-$  or an extended bromine chain) and the amount of the charge transfer from the  $(\text{SN})_x$  chains to the bromine. In addition, the polarization dependence of the Raman experiments indicated that the bromine molecular species was aligned parallel to the  $b$  axis of the  $(\text{SN})_x$  crystals.

As anisotropy in two-dimensional systems such as the layered compounds and intercalated compounds has been studied in EXAFS experiments by others [24, 25], we intend to extend these studies to systems of quasi one-dimensional geometry. The orientational anisotropy of the bromine molecules in the  $(\text{SN})_x$  host lattice provides an additional experimental parameter to study existing EXAFS theories [26]. In high symmetry (cubic) systems the intrinsic anisotropy of the X-ray absorption process, arising from the dipole nature of the relevant transition operator between the initial K-shell (1s) and final bound (excitonic) or free-electron state of p-character, is averaged out by the symmetric arrangement of atoms in the solid for unpolarized X-radiation. Due to the highly polarized nature of synchrotron radiation, we expect the anisotropy of the absorption cross-section to manifest itself by a  $\cos^2\theta$  dependence for rotated samples. Here  $\theta$  is the angle between the X-ray polarization vector and the  $b$  axis, and corresponds to rotating the sample by this angle about an axis perpendicular to the polarization vector and sample  $b$  axis. In Fig. 1(a) and (b) we present the X-ray absorption cross-section per atom in the 12 - 13.5 keV region with the X-ray polarization vector parallel and perpendicular to the sample  $b$  axis at room temperature and 5 K, respectively. The dramatic change in the white line feature [27] just below the onset of the bromine K-edge continuum transition is clearly seen. The detailed edge structure is shown on an expanded energy scale in Fig. 2, where we have also included the reference compound  $\text{S}_4\text{N}_3\text{Br}_3$  for comparison. The lowest energy transition seen most prominently in the fully aligned  $(\text{SNBr}_{0.4})_x$  ( $\vec{e} \parallel b$ ) sample arises from a 1s - 4p antibonding  $\pi^*$  state transition in the bromine molecule. The second-edge peak of lower

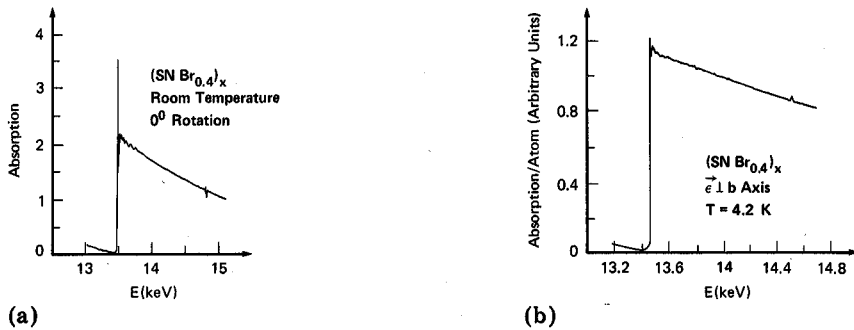


Fig. 1. (a) X-ray absorption around the Br K-edge at room temperature with  $\vec{\epsilon} \parallel b$  in brominated  $(\text{SN})_x$ . (b) X-ray absorption around the Br K-edge at 4.2 K with  $\vec{\epsilon} \perp b$  in brominated  $(\text{SN})_x$ .

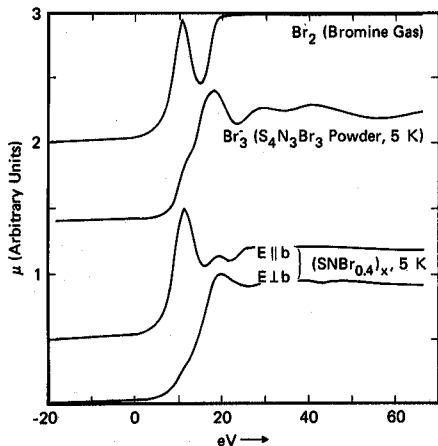
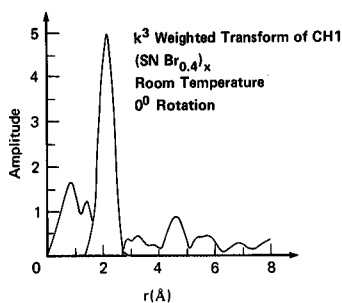


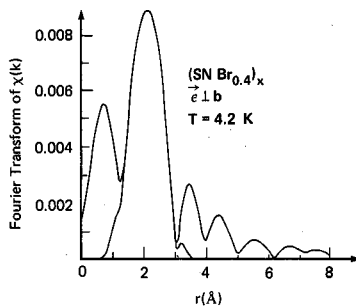
Fig. 2. Expanded Br edge structure for  $\text{Br}_2$ ,  $\text{S}_4\text{N}_3\text{Br}_3$  and brominated  $(\text{SN})_x$  with  $\vec{\epsilon} \parallel b$  and  $\vec{\epsilon} \perp b$  at 5 K.

intensity is interpreted as due to excitation into higher lying (5p,6p,...) valence states, consistent with its dominance in the perpendicularly oriented sample, in which the  $4p_x$ ,  $p_y$  orbitals are fully occupied. Here the intramolecular axis of the molecule has been defined as the quantization axis of the atomic orbitals.

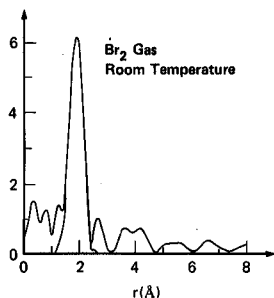
The most important information for the determination of the molecular species is the Br-Br bond distances. They are obtained by isolating the oscillatory part of the X-ray absorption cross section and Fourier transforming the spectral information into configuration space [26]. The absolute value of the resulting transform is a measure of the number of atoms at distance  $r$  from the average source atom after correction for phase shifts on reflection and thermal and lattice disorder. In Fig. 3(a) - (c) we show the results of the



(a)



(b)



(c)

Fig. 3. (a) Fourier transform of the oscillatory part of the absorption cross-section for brominated  $(\text{SN})_x$  at room temperature,  $\vec{\epsilon} \parallel b$ . (b) Fourier transform of the oscillatory part of the absorption cross-section for brominated  $(\text{SN})_x$  at  $T = 4.2$  K,  $\vec{\epsilon} \perp b$ . (c) Fourier transform of the oscillatory part of the absorption cross-section for  $(\text{Br})_2$  gas at room temperature.

Fourier transform for Br gas and brominated  $(\text{SN})_x$  with  $\vec{\epsilon} \parallel b$ ,  $\vec{\epsilon} \perp b$ . The presence of  $\text{Br}_3^-$  is clearly indicated from both the position of the first neighbor peak at 2.55 Å and the presence of a second neighbor peak at 5.0 Å. The size of the second nearest neighbor peak suggests strongly that multiple scattering corrections for this linear molecule play an important role [28]. This makes the determination of coordination numbers a difficult problem as the multiple scattering of the central Br atom requires detailed knowledge of the electron-Br forward scattering amplitude, which is presently not available. We have collected the temperature dependence of first and second neighbor Br distances in Table 1 and present coordination numbers uncorrected for multiple scattering in Table 2. We conclude that the predominant species in brominated  $(\text{SN})_x$  is  $\text{Br}_3^-$  or a larger  $\text{Br}_{2n+1}^-$  chain.

We note that coordination numbers and their ratios for any Br species can be determined by a counting argument. In Table 3 we present these theoretical coordination numbers and their ratios for  $n = 2, 3, 5, \infty$  and note that the results of Table 2 are not compatible with any of these predictions. A large  $\text{Br}_2$  component can, however, be ruled out on the basis of the absence of a broad first-shell peak (Fig. 3(a)). More refined data analysis may lead to

TABLE 1  
Summary of transform results for brominated (SN)<sub>x</sub>

First Shell			Second Shell				
Sample	Position R <sub>1</sub>		Amplitude A <sub>1</sub>	Position R <sub>2</sub>		Amplitude A <sub>2</sub>	A <sub>2</sub> /A <sub>1</sub>
Br <sub>2</sub> gas	1.93		203	—		—	
Br on (SN) <sub>x</sub> (86 K)	2.15	(2.55)	363	4.60	(4.95)	103	0.28
Br on (SN) <sub>x</sub> (150 K)	2.15	(2.55)	275	4.62	(4.97)	68	0.25
Br on (SN) <sub>x</sub> (300 K)	2.13	(2.53)	162	4.58	(4.93)	42	0.26

Br<sub>2</sub> gas Measured Br-Br = 2.28 Å Therefore  $\delta = 2.28 - 1.93 = 0.35$  Å  
The transform range used was  $4 \text{ \AA} < k < 14 \text{ \AA}^{-1}$  and the ratio method was used to extract the coordination numbers. The uncertainty in the first shell Br peak is  $\pm 0.02$  Å and  $\pm 0.1$  Å for the second shell.

TABLE 2

	300 K	150 K	86 K
First neighbor coordination *number $N_1$	$0.7 \pm 0.1$	$0.7 \pm 0.1$	$0.7 \pm 0.1$
Ratio of second neighbor coordination number $N_2$ to $N_1$ $\frac{N_2}{N_1} =$	$0.34 \pm 0.2$	$0.56 \pm 0.2$	$0.41 \pm 0.2$

\*Apart from the multiple scattering corrections discussed in the text, a very recent re-examination of EXAFS amplitudes for bromine gas standards has been made, which may affect the values given. (S. Heald and E. Stern, preprint 1979.)

TABLE 3

	$N_1$	$N_2$	$\rho = N_2/N_1$
Br <sub>2</sub>	1.0	0	0
Br <sub>3</sub>	1.33	0.67	0.5
Br <sub>5</sub>	1.6	1.2	0.75
Br <sub>∞</sub>	2.0	2.0	1.0

$N_1, N_2$  are the average first and second nearest neighbor coordination numbers.

further insight on small Br<sub>2</sub> admixtures as has recently been demonstrated for bromine adsorbed and intercalated in graphite [29], a system which has been investigated by X-ray absorption for several years. In regard to intermolecular bromine distances, it is clearly seen from Fig. 3(a) that no close Br-Br van der Waals distances are seen, suggesting isolated Br molecules or an extended chain. Additionally, analysis of the Br-S scattering for samples

with the  $b$  axis oriented perpendicular to X-ray polarization vector shows a very broad peak around 3.3 Å, indicative of a distribution of Br-S distances, and not a well defined Br-S distance as expected for a specific binding site.

### 3. The As K-edge in $\text{AsF}_5$ doped $(\text{CH})_x$

Among the recently studied conducting polymers,  $(\text{CH})_x$  in its undoped and doped forms has the widest base of appeal. This is due to its considerable interest as the prototypical organic conductor (polyenes have been studied as model systems for some 40 years [30, 31]), as well as for its potential for future applications due to its relative ease of fabrication, low cost, and stability [32, 33].

In contrast to the anisotropic three-dimensional conducting polymer  $(\text{SN})_x$  described in Section 2, pristine  $(\text{CH})_x$  is insulating due to the screw-axis symmetry of the polymer chain. Recent work at the University of Pennsylvania and our laboratory has shown, however, that both donor and acceptor doping induce 8 - 10 order of magnitude changes in the conductivity at the 1 - 2% dopant level [34, 35].

The X-ray absorption experiments described here have concentrated on the  $\text{AsF}_5$  doped  $(\text{CH})_x$  system. Here, too, as in the case of brominated  $(\text{SN})_x$ , close parallels exist with another intercalated graphite system discussed in this Conference [36]. Bartlett *et al.* [13] have extensively studied the  $\text{AsF}_5$ -doped graphite system by X-ray absorption techniques, and we have recently proposed the same solid state reaction, *i.e.*,  $3\text{AsF}_5 \rightarrow 2\text{AsF}_6^- + \text{AsF}_3$  to occur in the  $(\text{CH})_x$  polymer [14]. Only preliminary experiments have been performed to date due to limited access to high energy beam time at the Stanford Linear Accelerator Synchrotron Radiation Laboratory. The As K-edge at 11.9 keV is employed as the tool for edge structure and EXAFS measurements. Our goal is very similar to that reported on in the previous Section, namely, the identification of the dominant  $\text{AsF}_n$  ( $n = 3, 5, 6, ?$ ) species responsible for the drastic change in transport properties, the relative position and orientation of the incorporated  $\text{AsF}_n$  relative to the  $(\text{CH})_x$  chains and the amount of charge transfer and temperature dependence of all measured parameters.

In Fig. 4 we show a typical absorption spectrum in the 11.6 - 13.0 keV energy region of the As K-edge in  $(\text{CH})_x$  at 86 K. Once again, very prominent white line features are evident below the edge, whose origin will be discussed in Section 4. We have also used standards of  $\text{AsF}_5$  gas and  $\text{AsF}_3$  gas at room temperature to derive the appropriate phase shift correction from the known As-F distance in the  $\text{AsF}_5$  molecule [37]. Figures 5 and 6 present the Fourier transforms of the oscillatory part of the absorption cross section for  $\text{AsF}_5$  gas phase molecules and  $\text{AsF}_5$ -doped  $(\text{CH})_x$ . The transform range is limited to a smaller range of wavevectors ( $K < 10 \text{ \AA}^{-1}$ ) due to fluorine as compared with the bromine backscattering. Nevertheless, the peak positions are not strongly affected by this feature, and we report a preliminary value of 1.82 Å

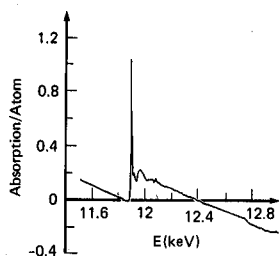


Fig. 4. X-ray absorption around the As K-edge at  $T = 86$  K in  $\text{AsF}_5$ -treated  $(\text{CH})_x$ .

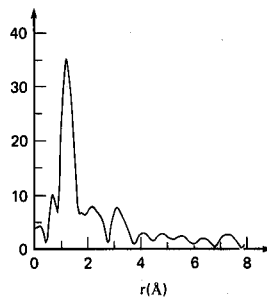


Fig. 5. Fourier transform of the oscillatory part of the absorption cross-section for  $\text{AsF}_5$ -treated  $(\text{CH})_x$  at 86 K.

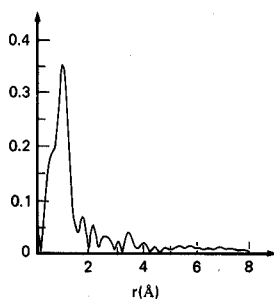


Fig. 6. Fourier transform of the oscillatory part of the absorption cross-section for  $\text{AsF}_5$  gas at room temperature.

for the average As-F distance in  $(\text{CH})_x^*$ . No reliable coordination numbers have been obtained from the data obtained to date. We note that the As-F distances for  $\text{AsF}_3$ ,  $\text{AsF}_5$  and  $\text{AsF}_6^-$  molecules are all in the range of 1.68 - 1.73 Å so that no definite assignment can be made on the basis of the preliminary results presented. It is hoped that future measurements will allow the determination of the fluorine coordination number to confirm the suggested presence of  $\text{AsF}_6^-$  in  $(\text{CH})_x$ . It does not seem that photoemission experiments on the same material [15], which have been interpreted to show the presence of the  $\text{AsF}_5$  species in the  $(\text{CH})_x$  polymer, can compete with the X-ray absorption measurements due to their limitation to the surface regions. It is conceivable, however, that  $\text{AsF}_5$  does reside in surface regions, while the solid state reaction takes place in the bulk of the material, providing a way of reconciling the two different sets of experiments. The advantage of the X-ray absorption experiments used by us lies in their bulk nature and relative simplicity of execution and interpretation.

\*As these data are derived from a small number of samples, we do not attach great significance to the 0.1 Å increase in the average As-F bond length at this stage.



#### 4. Excitonic edge structure in $\text{AsF}_3$ , $\text{AsF}_5$ and $\text{AsF}_6^-$

We have discussed in some detail in the preceding Section the main goal of this work: the identification of molecular species in a polymeric and partially disordered environment. The emphasis in the first three Sections has been on the use of structural information such as nearest neighbor distances and coordination numbers obtained from the EXAFS region of the spectrum, which conventionally is defined from about 50 eV above the edge of the threshold to the disappearance of oscillations in the absorption some 1 000 - 1 500 eV above the edge, depending on the material.

In this Section we review the energy region immediately below the edge, in which the X-ray photon induces transitions from the 1s core state to a bound (excitonic) final state of p-like symmetry. In particular, we discuss the very interesting possibility of utilizing the different 1s hole-final state electron states of the different molecules  $\text{AsF}_n$  ( $n = 3, 5, 6$ ) as a means of identifying the molecular species.

To this end, SCF Hartree-Fock calculations have been performed on the molecules mentioned [38]. This calculation will be reported in detail elsewhere [39]. We confine ourselves here to sketching the physics of the states involved and indicate the results obtained and their implications for the interpretation of the edge structure in  $(\text{CH})_x$ .

The notion of inner and outer well states in the interpretation of the core level bound state and continuum transitions was proposed in ref. 40. The model of a spherical potential due to a 1s core hole and a repulsive barrier in the region of the electronegative fluorines suggests the existence of valence-like states inside the spherical barrier of the fluorine cage, as well as weakly bound Rydberg states with the dominant portion of the electronic wavefunction outside the molecule and, hence, subject to an approximately spherically-symmetric Coulomb potential. In addition, this kind of model predicts resonance states in the continuum corresponding to quasi-bound electronic states inside the barrier with finite widths due to the coupling to the continuum states available outside the Coulomb barrier of the fluorine cage. These later states are not accessible to our calculational approach, which utilizes bound Gaussian basis sets.

The calculations we have performed are the first of their kind [41] for the  $\text{AsF}_n$  series and offer a quantitative approach to the study of the edge-structure of systems with large numbers of electrons. They fully take account of relaxation effects in the various shells due to the removal of an electron from the 1s shell and the filling of a virtual orbital by the electron removed. The binding energies for the various final states of p-like symmetry are calculated by taking the difference of the ionization energy corresponding to the electron being removed to infinity and the energy with a 1s core hole and the electron in one of the virtual orbitals. Typical binding energies are in the range 2 - 10 eV for the molecules studied [38, 39].

Within the finite size basis set we have used, we identify three bound states for  $\text{AsF}_5$ , one valence, the other two Rydberg states, while there are

four bound states in  $\text{AsF}_3$ . In  $\text{AsF}_6^-$ , however, no bound states have been found, suggesting that the very strong white line feature seen in all these three systems preserves its large oscillator strength when pushed into the continuum.

It is clear that detailed information on the number, energies, and oscillator strengths of bound state transitions in this group of molecules will lend considerable confidence to the assignment of the near edge spectrum of  $\text{AsF}_5$ -doped  $(\text{CH})_x$ . Of decisive importance is the calculational result that the transitions in the different molecules are non-overlapping due to differences in the ionization energies, and typical splittings for states are 2 - 3 eV. This is sufficient to resolve these states despite the intrinsic 1s core hole width of 2 eV and an additional instrumental broadening of 1.5 eV.

## 5. Summary and conclusion

This paper has presented the first successful application of X-ray absorption measurements in the energy region of 11 - 14 keV, corresponding to the As and Br K-edge to the determination of molecular structure in the conducting polymers brominated  $(\text{SN})_x$  and  $\text{AsF}_5$ -doped  $(\text{CH})_x$ .

We have demonstrated that the bulk nature of X-ray absorption gives direct information on Br nearest and second nearest neighbor distances from an analysis of the EXAFS region. The dominant bromine species in  $(\text{SN})_x$  has been identified on this basis as  $\text{Br}_3^-$  although a more extended bromine chain cannot be excluded at this time from the analysis.

Preliminary results for  $\text{AsF}_5$  treated  $(\text{CH})_x$  are presented, which indicate slightly larger As-F distances than found in  $\text{AsF}_5$  gas phase molecules. Detailed SCF calculations on the bound state region below the ionization limit for K-shell excitation are reported for the molecules  $\text{AsF}_3$ ,  $\text{AsF}_5$  and  $\text{AsF}_6^-$ , all of which have been considered to be present in  $(\text{CH})_x$ . These calculations provide promise for definite assignment of the observed edge features in  $\text{AsF}_5$  treated  $(\text{CH})_x$ . In addition, the computational results on these bound states provide interesting information on electron-deep hole excitations of cage molecules with inner and outer well character, which will contribute to a better understanding of the dopant-host polymer interactions.

The most attractive feature of X-ray absorption experiments is the simplicity of addressing a particular atom (ion), in systems such as the doped organic polymers or graphite, by exciting its K-shell electrons and employing the resulting weakly bound or quasi-free electron as a probe of the immediate vicinity of the excited atom (ion). As the incident energy of the X-ray is varied continuously by the monochromator, using a synchrotron radiation source, the technique allows the use of electrons bound by a few eV relative to their ionization energy up to kinetic energies of 1.5 keV. As the absorption process takes place in the bulk of the medium the only requirement on sample preparation is uniform (pin-hole free) sample thickness of the order of an absorption length, typically, a few microns or larger depending on the

absorber concentration. We expect that the technique of X-ray absorption spectroscopy utilizing both the near-edge and EXAFS region will provide an important tool in the more detailed understanding of polymeric conductors in the future.

From the theoretical point of view, several topics require future work: the effect of multiple scattering in finite chain systems based on reliable electron-atom forward scattering amplitudes, and the calculation of resonant transitions in the low energy continuum range (between 0 and 50 eV above the edge) are the most important ones for the system we have studied.

### Acknowledgments

This work was partially supported by NSF grant No. DMR77-08695 and by NSF grant No. DMR77-07692, in cooperation with the Stanford Linear Accelerator Center and the U.S. Department of Energy.

### References

- 1 H. Morawitz, W. D. Gill, P. M. Grant, G. B. Street and D. Sayers, *Bull. Am. Phys. Soc.*, 23 (1978) 304; H. Morawitz, W. D. Gill, P. M. Grant, G. B. Street and D. Sayers, in S. Barisic, A. Bjelis, C. Cooper and B. Leontic (eds.), *Proc Conf. on Quasi One-Dimensional Conductors*, Dubrovnik, 1978, *Lecture Notes in Physics*, Springer, Berlin, 1979.
- 2 T. C. Clarke, W. D. Gill, P. M. Grant, H. Morawitz, G. B. Street and D. Sayers, *Bull. Am. Phys. Soc.*, 23 (1978) 344.
- 3 R. L. Greene and G. B. Street, in H. J. Keller (ed.), *Chemistry and Physics of One-Dimensional Metals*, Plenum Publishing Company, New York, 1977.
- 4 H. Shirakawa, E. J. Louis, A. G. MacDiarmid, C. K. Chiang and A. J. Heeger, *Chem. Commun.*, (1978) 578.
- 5 W. D. Gill, T. C. Clarke and G. B. Street, *Bull. Am. Phys. Soc.*, 24 (1979) 327; J. Kwak, T. C. Clarke, R. L. Greene and G. B. Street, *Solid State Commun.*, in press.
- 6 A. Bienenstock, H. Winick and S. Doniach, *Stanford Synchrotron Radiation Lab. Activity Rep. 78/02*, May 1978.
- 7 G. N. Kulipanov and A. N. Skriskii, *Sov. Phys. Usp.*, 20 (1978) 559.
- 8 D. Sayers, E. A. Stern and F. Lytle, *Phys. Rev. Lett.*, 34 (1975) 1361.
- 9 P. Eisenberger and B. M. Kincaid, *Chem. Phys. Lett.*, 36 (1975) 134.
- 10 S. N. Hunter and A. Bienenstock, *Proc. 6th Int. Conf. Amorphous and Liquid Semiconductors*, Leningrad, 1975.
- 11 *Proc. Int. Conf. Intercalation Compounds of Graphite*, *Mater. Sci. Eng.*, 31, December, 1977.
- 12 G. M. Foley, C. Zeller, E. R. Faraldealu and F. L. Vogel, *Solid State Commun.*, 24 (1977) 371.
- 13 N. Bartlett, R. N. Biagioni, B. U. McQuillan, A. S. Robertson and A. C. Thompson, *J. Chem. Soc., Chem. Commun.*, (1978) 200.
- 14 T. C. Clarke, R. H. Geiss, W. D. Gill, P. M. Grant, J. W. Macklin, H. Morawitz, J. Rabolt, D. Sayers and G. B. Street, *J. Chem. Soc., Chem. Commun.*, (1979) 332.
- 15 W. R. Salaneck, H. R. Thomas, C. B. Duke, E. W. Plummer, A. J. Heeger and A. G. MacDiarmid, *J. Chem. Phys.*, in press, and *Synthetic Metals*, 1 (1979/80) 133.
- 16 N. Bartlett, B. McQuillan and A. S. Robertson, *Mater. Res. Bull.*, 13 (1978) 1259.

- 17 S. H. Hunter, *SSRP Rep. 77/04*, March 1977, *Ph.D. Thesis*, Stanford University, 1977.
- 18 S. M. Heald and E. A. Stern, *Phys. Rev. B*, 16 (1977) 5 579.
- 19 J. J. Mayerle, G. Wolmershaeuser and G. B. Street, *Inorg. Chem.*, 17 (1978) 2 685.
- 20 G. B. Street, W. D. Gill, R. Geiss, R. L. Greene and J. J. Mayerle, *Chem. Commun.*, (1977) 407.
- 21 W. D. Gill, W. Bludau, R. H. Geiss, P. M. Grant, R. L. Greene, J. J. Mayerle and G. B. Street, *Phys. Rev. Lett.*, 38 (1977) 1 305.
- 22 H. Temkin and G. B. Street, *Solid State Commun.*, 25 (1978) 455.
- 23 J. W. Macklin, G. B. Street and W. D. Gill, *J. Chem. Phys.*, 70 (1979) 2 425.
- 24 E. A. Stern, D. Sayers and F. W. Lytle, *Phys. Rev. Lett.*, 37 (1976) 298.
- 25 G. Beni and P. M. Platzmann, *Phys. Rev. B*, 14 (1976) 1 514.
- 26 E. A. Stern, *Phys. Rev. B*, 10 (1974) 3 027; C. A. Ashley and S. Doniach, *Phys. Rev. B*, 11 (1975) 1 279; P. A. Lee and J. P. Pendry, *Phys. Rev. B*, 11 (1975) 2 795.
- 27 M. Brown, R. E. Peierls and E. A. Stern, *Phys. Rev. B*, 15 (1977) 738.
- 28 J. J. Rehr and E. A. Stern, *Phys. Rev. B*, 14 (1976) 4 413.
- 29 S. Heald and E. A. Stern, *Synthetic Metals*, 1 (1979/80) 249.
- 30 C. A. Coulson, *Proc. R. Soc. London, Ser. A*, 164 (1938) 383.
- 31 H. Kuhn, *J. Chem. Phys.*, 16 (1948) 840; H. C. Longuet-Higgins and L. Salem, *Proc. R. Soc. London, Ser. A*, 251 (1959) 172.
- 32 G. B. Street and W. D. Gill, in W. E. Hatfield (ed.), *Molecular Metals*, Plenum Publishing Co., 1979.
- 33 G. B. Street and T. C. Clarke, *Annals of Chemistry*, in press.
- 34 N. Bartlett, E. M. McCarron, B. W. McQuillan and T. E. Thompson, *Synthetic Metals*, 1 (1979/80) 221.
- 35 C. K. Chiang, Y. W. Park, A. J. Heeger, H. Shirakawa, E. J. Louis and A. G. MacDiarmid, *J. Chem. Phys.*, 69 (1978) 5 098.
- 36 J. F. Kwak, W. D. Gill, R. L. Greene, K. Seeger, T. C. Clarke and G. B. Street, *Synthetic Metals*, 1 (1979/80) 213.
- 37 F. B. Clippard, Jr. and L. S. Bartell, *Inorg. Chem.*, 9 (1970) 805.
- 38 P. Bagus and H. Morawitz, *Bull. Am. Phys. Soc.*, 24 (1979) 446.
- 39 H. Morawitz and P. Bagus, to be published.
- 40 B. Cadioli, U. Pincelli, E. Tosatti, U. Fano and J. L. Dehmer, *Chem. Phys. Lett.*, 17 (1972) 15.
- 41 Calculations on the edge structure of  $\text{GeCl}_4$  using the scattered wave  $X_\alpha$  method have recently been reported. D. Misemer, R. Natoli and S. Doniach, to be published.